Bioorganic & Medicinal Chemistry Letters 21 (2011) 1472–1475

Contents lists available at ScienceDirect

Bioorganic & Medicinal Chemistry Letters

journal homepage: www.elsevier.com/locate/bmcl

Synthesis of cell-permeable stapled peptide dual inhibitors of the p53-Mdm2/Mdmx interactions via photoinduced cycloaddition

Michael M. Madden [a], Avinash Muppidi [a], Zhenyu Li [b], Xiaolong Li [b], Jiandong Chen [b,*], Qing Lin [a,*]

[a] Department of Chemistry, State University of New York at Buffalo, Buffalo, NY 14260, USA
[b] Department of Molecular Oncology, H. Lee Moffitt Cancer Center, Tampa, FL 33612, USA

ARTICLE INFO

Article history:
Received 26 November 2010
Revised 27 December 2010
Accepted 3 January 2011
Available online 7 January 2011

Keywords:
Inhibitors
Protein–protein interaction
Dipolar cycloaddition
Cellular uptake
Stapled peptides

ABSTRACT

We report the first application of a photoinduced 1,3-dipolar cycloaddition reaction to 'staple' a peptide dual inhibitor of the p53-Mdm2/Mdmx interactions. A series of stapled peptide inhibitors were efficiently synthesized and showed excellent dual inhibitory activity in ELISA assay. Furthermore, the positively charged, stapled peptides showed enhanced cellular uptake along with modest in vivo activity.

The α-helix is one of the most common secondary structural elements in proteins; approximately 40% of amino acids in proteins are found as part of α-helices.[1] Furthermore, α-helices frequently mediate the protein–protein interactions that regulate diverse cellular processes.[2] Whereas short peptides may exhibit potent in vitro activity and are generally devoid of toxicity, they are rarely good drug candidates for intracellular targets because of their unfavorable pharmacological properties, for example, low proteolytic stability and inefficient cellular uptake. While the peptide side-chain cross-linking through disulfide bond[3] and lactam formations[4] were known long ago to increase the helicity and proteolytic stability of peptides, the hydrocarbon stapling—direct cross-linking of peptide side-chains via ring-closing metathesis—has emerged as one of the most promising strategies reported to date.[5] Despite its tremendous success, alternative stapling methods other than hydrocarbon stapling are still desirable because they may offer stapled peptides with distinct physicochemical properties. We recently reported a photoinduced 1,3-dipolar cycloaddition based stapling reaction for a model 3_{10} helical peptide carrying the tetrazole and alkene moieties, affording enhanced peptide cell permeability.[6] Here we report the application of this stapling chemistry to dual-active peptide inhibitors of p53-Mdm2/Mdmx interactions and the characterization of the inhibitory activities of the stapled peptides both in vitro and in cancer cells.

The p53 tumor suppressor is a potent inducer of cell cycle arrest, apoptosis, cellular senescence, and innate immunity. It is activated in response to oncogenic transformation, extrinsic stress, and viral infection to protect higher organisms from cancer. Mdm2 and Mdmx function as two key regulators of p53 by binding to its N-terminus, inhibiting its transcriptional activity, and promoting its degradation. Despite sharing high sequence and structural homology, Mdm2 and Mdmx regulate p53 in distinct manners. Mdm2 serves as an E3 ligase and downregulates p53 activity by promoting p53 ubiquitination and subsequent degradation.[7] In contrast, Mdmx abrogates p53 function by sequestering it into the inactive p53–Mdmx complex.[8] Both Mdm2 and Mdmx are overexpressed in human cancers, making them attractive anticancer drug targets.[9] However, despite their prominent roles in cancer progression, potent dual-active small molecules that disrupt both p53-Mdm2 and p53-Mdmx interactions have not been reported. By screening a phage library, we have recently discovered a potent peptide dual inhibitor (PDI) of the p53-Mdm2/Mdmx interactions with the sequence of LTFEHYWAQLTS.[10] However, PDI was found to be cell-impermeable, preventing its further development into therapeutics. To overcome this limitation, we hypothesized that by applying our photoinduced stapling chemistry,[6] we could obtain cell-permeable analogs that retain dual inhibitory activity.

To identify suitable sites in the PDI sequence to append the alkene and tetrazole moieties, we first performed an acetyllysine scan and found that Glu-4, His-5, Ala-8, Gln-9, and Thr-11 can be substituted without significant loss in activity (Table S2 in Supplementary data). This finding is consistent with the crystal structures of PDI in complexes with Mdm2 and Mdmx, in which these five

* Corresponding authors.
E-mail addresses: jiandong.chen@moffitt.org (J. Chen), qinglin@buffalo.edu (Q. Lin).

0960-894X/$ - see front matter © 2011 Elsevier Ltd. All rights reserved.
doi:10.1016/j.bmcl.2011.01.004

residues are solvent exposed and do not make critical contacts with either Mdm2 or Mdmx (Fig. 1a).[11] After mapping these residues to the PDI helix wheel model (Fig. 1b), three possible stapling schemes emerged: *i*,*i*+4 stapling between Glu-4 and Asp-8 and between His-5 and Gln-9, and *i*,*i*+7 stapling between Glu-4 and Thr-11.[12] To expedite the synthesis of stapled peptides, alkene-(α) and tetrazole-modified lysine (β) were prepared from Fmoc-Lys-OH (Scheme S1 in Supplementary data) and used directly in solid-phase peptide synthesis. After cleavage from the resin and purification by reverse-phase HPLC, linear peptides were exposed to a handheld UV lamp (UVM-57, 302 nm, 115 V, 0.16 A) in a mixed acetonitrile/water (1:1) solvent for 2 h (Scheme 1). Three stapled peptides, **1**–**3**, embodying three stapling patterns were obtained (Table 1). The conversions from linear precursors to stapled products were 82% for **1**, 75% for **2**, to 89% for **3**, based on HPLC analysis (Figs. S1–S3 in Supplementary data).

Previously, PDI was determined to inhibit the full-length p53 binding to Mdm2 and Mdmx with IC_{50} values of 44 nM and 550 nM, respectively, in an ELISA assay.[11b] To gauge the effect of stapling on inhibitory activity, stapled PDI analogs **1**–**3** were evaluated and their inhibitory activity data were collected in Table 1. Compared to PDI, **1** with the cross-linker connecting residues 4–8 showed similar activities against both Mdm2 and Mdmx. The other *i*,*i*+4 stapled PDI analog **2** with the cross-linker connecting residues 5–9 showed roughly fourfold drop in Mdm2 activity and threefold drop in Mdmx activity. Meanwhile, the *i*,*i*+7 stapled PDI analog **3** showed sevenfold increase in Mdm2 activity together with a slight improvement in Mdmx activity. To discern the effect of stapling from that of residue substitution, we determined the activity of its linear precursor, PDI-4α11β, with IC_{50} values of 1200 nM and 6300 nM against Mdm2 and Mdmx, respectivley. By comparing the activity of **3** with that of PDI-4α11β, stapling led to roughly

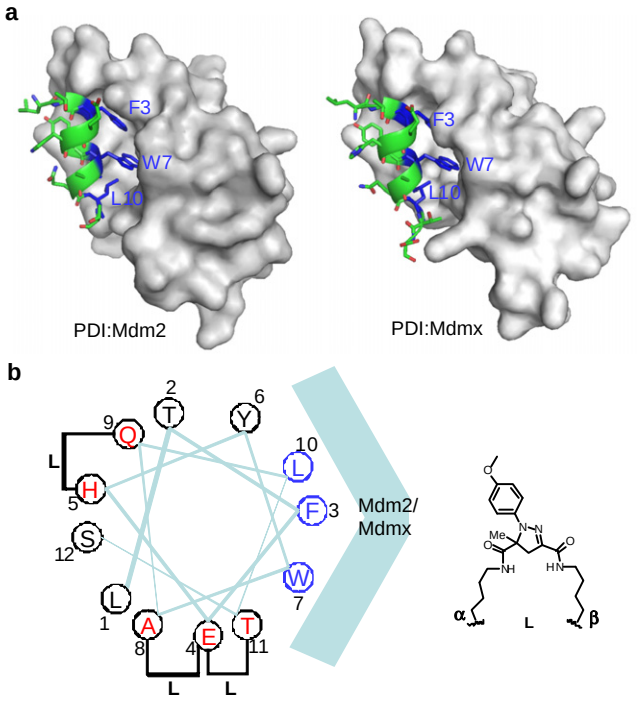

Figure 1. (a) Crystal structures of PDI bound to Mdm2 (PDB code: 3G03) and Mdmx (PDB code: 3FDO). The proteins were rendered in surface model and PDI was shown in ribbon and tube model. The side chains of three canonical residues, F3, W7 and L10, were shown in blue. (b) Helical wheel diagram of PDI viewed from the N- to C-terminus. The five possible stapling sites were colored in red. The pyrazoline cross-linker structure formed after the cycloaddition reaction is shown on the right.

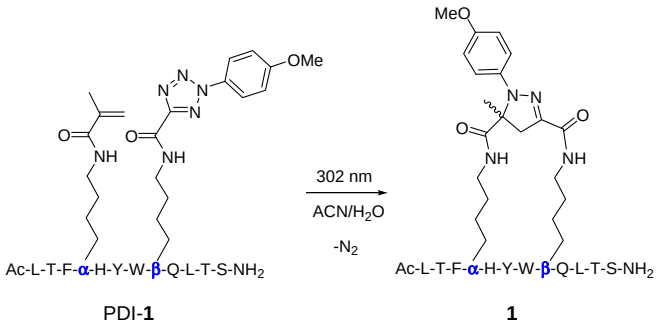

Scheme 1. Representative synthesis of stapled peptide **1** using a photoinduced 1,3-dipolar cycloaddition reaction. α and β denote the alkene and tetrazole-modified lysine, respectively.

200-fold increase in the Mdm2 activity and 20-fold increase in the Mdmx activity.

Since higher positive charges generally lead to improved cellular uptake,[5d,13] we prepared a series of positively charged PDI analogs by substituting the remaining non-essential residues (His-5, Ala-8, Gln-9 and Thr-11) in **1** and **3** with either one (**1a**, **3a** and **3b**) or two arginines (**1b**, **3c** and **3d**) and determined their inhibitory activities (Table 1). Compared to their parent peptides, these positively charged analogs showed 2–6-fold drop in activity against Mdm2 and small changes against Mdmx (Table 1), indicating that arginine substitutions were largely tolerated. Furthermore, we probed the effect of increased hydrophobicity at the binding surface of PDI by replacing the canonical Trp with 6-chlorotryptophan to derive **3e**.[14] Interestingly, **3e** showed roughly twofold increase in Mdm2 activity but twofold decrease in Mdmx activity relative to **3d** (Table 1), which can be attributed to the interaction between 6-chlorine and Phe-86 of Mdm2, but not Mdmx, as detected previously.[14b]

To examine whether stapled PDI analogs penetrate into cancer cells, we took advantage of the intrinsic fluorescence of the pyrazoline cross-linker[6] and monitored their cellular uptake by fluorescence microscopy. Our initial study revealed that the charge neutral stapled peptide **3** was not cell-permeable (Fig. S6 in Supplementary data). To our delight, treatment of U2OS cells with +1 charged stapled peptides **3a** and **3b** gave rise to a punctuated fluorescence pattern (Fig. 2). This distribution pattern suggests that stapled peptides are taken up by cancer cells via a pinocytotic pathway where the majority of peptides are likely trapped in the endosomes.[15] On the other hand, treatment of U2OS cells with +2 charged stapled peptides **3c**, **3d** and **3e** produced more diffusive fluorescence patterns, suggesting that increased positive charge may facilitate the peptides to escape the acidic endosomes. Notably, stapled peptide **3c** in which two arginines form a continuous positive patch in an *i*,*i*+4 fashion showed a strong and uniform fluorescence distribution in the cytosol, indicating that the charge locations are also important in addition to the total charge. This charge location dependency also suggests that the observed intracellular fluorescence was not an artifact derived from the cell fixation. It is noteworthy that U2OS cells treated with a linear fluorescent peptide carrying +2 charge, **4** (see Table 1 for sequence), under identical conditions did not produce any intracellular fluorescence, confirming that stapling is essential for cellular uptake (Fig. 2). In our preliminary circular dichroism study, stapled peptide **3e** showed 21% helicity compared to 13% for peptide **4** of the same sequence (Fig. S7), indicating that stapling indeed increases helicity, which is partly responsible for the enhanced cellular uptake.

To assess whether enhanced cellular uptake imparts in vivo activity, U2OS cells stably expressing a p53-dependent luciferase

Table 1
Sequences and inhibitory activity of PDI analogs[a]

Name	Sequence	Charge	IC_{50}, Mdm2 (nM)	IC_{50}, Mdmx (nM)
Nutlin-3[b]			600	No activity
PDI	LTFEHYWAQLTS[c]	−1	44	550
1	LTFαHYWβQLTS	0	61 ± 5.2	540 ± 55
1a	LTFαHYWβ**R**LTS	+1	71 ± 3.9	220 ± 19
1b	LTFαHYWβ**R**L**R**S	+2	160 ± 8.6	390 ± 25
2	LTFEαYWAβLTS	−1	170 ± 15	1600 ± 290
3	LTFαHYWAQLβS	0	6.2 ± 1.5	340 ± 27
3a	LTFαHYWA**R**LβS	+1	15 ± 0.6	240 ± 18
3b	LTFαHYW**R**QLβS	+1	18 ± 0.9	210 ± 23
3c	LTFα**R**YWA**R**LβS	+2	39 ± 1.4	550 ± 58
3d	LTFα**R**YW**R**QLβS	+2	28 ± 1.0	410 ± 38
3e	LTFα**R**YW$_{Cl}$**R**QLβS[d]	+2	14 ± 1.2	810 ± 95
4	LTFK$_{Ac}$**R**YW**R**QLK$_{Pyr}$S[e]	+2	2300 ± 220	34,000

[a] ELISA assays were repeated three times in deriving average IC_{50} values along with standard deviations.
[b] IC_{50} values were taken from Ref. 10 where the same ELISA assays were performed.
[c] Residues tolerant of substitution were underlined.
[d] W_{Cl} = 6-chlorotryptophan.
[e] K_{Ac} = N^{ε}-acetyllysine; K_{pyr} = N^{ε}-pyrazolinelysine, see Table S1 in Supplementary data for structure.

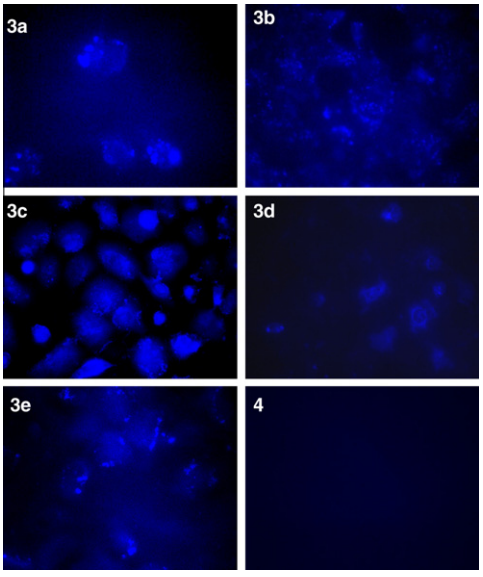

Figure 2. Fluorescence images of fixed U2OS cells after treatment with 20 μM of stapled PDI-**3a–e** or linear PDI-**4** for 4 h at 37 °C. A 20× oil immersion lens was used.

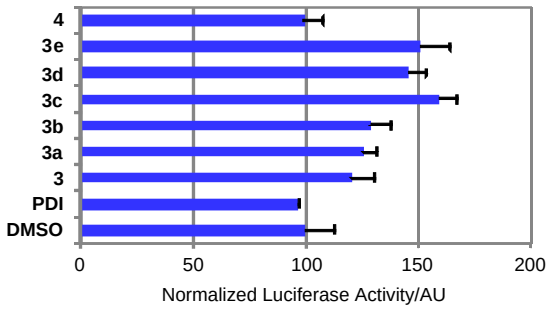

Figure 3. The p53-dependent luciferase transcriptional activation in U2OS cells: The luciferase activities were measured at least three times and the averaged activities along with standard deviations were plotted.

reporter were treated with 20 μM of stapled peptides along with the linear control peptides PDI and **4**. We found that compared to the linear control peptides which were inactive in this assay, all positively charged stapled peptides showed modest, yet reproducible activity in luciferase activation (Fig. 3). Stapled peptide **3c** showed the highest activity, giving rise to 1.6-fold increase in luciferase activation, which is in good agreement with its excellent cellular uptake (Fig. 2). By comparison, treatment of 5 μM of nutlin-3, a cell-permeable small-molecule Mdm2 inhibitor, gave rise to a fourfold increase in luciferase activation, higher than all the stapled peptides. Taken together, despite higher in vitro activity (Table 1), a large fraction of stapled peptides appear to get trapped in the endosomes and likely degraded before they can reach their targets.

In summary, we have demonstrated a facile synthesis of stapled peptide dual inhibitors of the Mdm2/Mdmx interactions using a photoinduced cycloaddition reaction. Compared to PDI, stapled PDIs showed significantly higher inhibitory activities: up to sevenfold against Mdm2 and 2.5-fold against Mdmx. The inhibitory activity was found to depend on stapling site, charge number and distribution, and overall hydrophobicity. Moreover, the positively charged, stapled peptides showed enhanced cellular uptake along with modest in vivo activity.

Acknowledgments

We gratefully acknowledge the Pardee Foundation and the National Institutes of Health (GM 085092 to Q.L.; CA 109636 and 118210 to J.C.) for financial support.

Supplementary data

Supplementary data associated with this article can be found, in the online version, at doi:10.1016/j.bmcl.2011.01.004.

References and notes

1. Kabsch, W.; Sander, C. *Biopolymers* **1983**, *22*, 2577.
2. (a) Meador, W. E.; Means, A. R.; Quiocho, F. A. *Science* **1992**, *257*, 1251; (b) Kussie, P. H.; Gorina, S.; Marechal, V.; Elenbaas, B.; Moreau, J.; Levine, A. J.; Pavletich, N. P. *Science* **1996**, *274*, 948; (c) Sattler, M.; Liang, H.; Nettesheim, D.; Meadows, R. P.; Harlan, J. E.; Eberstadt, M.; Yoon, H. S.; Shuker, S. B.; Chang, B. S.; Minn, A. J.; Thompson, C. B.; Fesik, S. W. *Science* **1997**, *275*, 983.
3. Jackson, D. Y.; King, D. S.; Chmielewski, J.; Singh, S.; Schultz, P. G. *J. Am. Chem. Soc.* **1991**, *113*, 9391.
4. (a) Bracken, C.; Gulyas, J.; Taylor, J. W.; Baum, J. *J. Am. Chem. Soc.* **1994**, *116*, 6431; (b) Phelan, C. J.; Skelton, N. J.; Braisted, A. C.; McDowell, R. S. *J. Am. Chem. Soc.* **1997**, *119*, 455; (c) Sia, S. K.; Carr, P. A.; Cochran, A. G.; Malashkevich, V. N.; Kim, P. S. *Proc. Natl. Acad. Sci. U.S.A.* **2002**, *99*, 14664; (d) Harrison, R. S.; Shepherd, N. E.; Hoang, H. N.; Ruiz-Gomez, G.; Hill, T. A.; Driver, R. W.; Desai, V. S.; Young, P. R.; Abbenante, G.; Fairlie, D. P. *Proc. Natl. Acad. Sci. U.S.A.* **2010**, *107*, 11686.

5. (a) Blackwell, H. E.; Grubbs, R. H. *Angew. Chem., Int. Ed.* **1998**, *37*, 3281; (b) Schafmeister, C. E.; Po, J.; Verdine, G. L. *J. Am. Chem. Soc.* **2000**, *122*, 5891; (c) Walensky, L. D.; Kung, A. L.; Escher, I.; Malia, T. J.; Barbuto, S.; Wright, R. D.; Wagner, G.; Verdine, G. L.; Korsmeyer, S. J. *Science* **2004**, *305*, 1466; (d) Bernal, F.; Tyler, A. F.; Korsmeyer, S. J.; Walensky, L. D.; Verdine, G. L. *J. Am. Chem. Soc.* **2007**, *129*, 2456; (e) Gavathiotis, E.; Suzuki, M.; Davis, M. L.; Pitter, K.; Bird, G. H.; Katz, S. G.; Tu, H. C.; Kim, H.; Cheng, E. H.; Tjandra, N.; Walensky, L. D. *Nature* **2008**, *455*, 1076; (f) Moellering, R. E.; Cornejo, M.; Davis, T. N.; Del Bianco, C.; Aster, J. C.; Blacklow, S. C.; Kung, A. L.; Gilliland, D. G.; Verdine, G. L.; Bradner, J. E. *Nature* **2009**, *462*, 182; (g) Bautista, A. D.; Appelbaum, J. S.; Craig, C. J.; Michel, J.; Schepartz, A. *J. Am. Chem. Soc.* **2010**, *132*, 2904.
6. Madden, M. M.; Rivera Vera, C. I.; Song, W.; Lin, Q. *Chem. Commun.* **2009**, 5588.
7. (a) Wu, X.; Bayle, J. H.; Olson, D.; Levine, A. J. *Genes Dev.* **1993**, *7*, 1126; (b) Levine, A. J. *Cell* **1997**, *88*, 323.
8. (a) Tanimura, S.; Ohtsuka, S.; Mitsui, K.; Shirouzu, K.; Yoshimura, A.; Ohtsubo, M. *FEBS Lett.* **1999**, *447*, 5; (b) Sharp, D. A.; Kratowicz, S. A.; Sank, M. J.; George, D. L. *J. Biol. Chem.* **1999**, *274*, 38189; (c) Linares, L. K.; Hengstermann, A.; Ciechanover, A.; Muller, S.; Scheffner, M. *Proc. Natl. Acad. Sci. U.S.A.* **2003**, *100*, 12009; (d) Shvarts, A.; Steegenga, W. T.; Riteco, N.; van Laar, T.; Dekker, P.; Bazuine, M.; van Ham, R. C.; Van der Houven, v. O. W.; Hateboer, G.; van der Eb, A. J.; Jochemsen, A. G. *EMBO J.* **1996**, *15*, 5349.
9. Toledo, F.; Wahl, G. M. *Nat. Rev. Cancer* **2006**, *6*, 909.
10. Hu, B.; Gilkes, D. M.; Chen, J. *Cancer Res.* **2007**, *67*, 8810.
11. (a) Czarna, A.; Popowicz, G. M.; Pecak, A.; Wolf, S.; Dubin, G.; Holak, T. A. *Cell Cycle* **2009**, *8*, 1176; (b) Phan, J.; Li, Z.; Kasprzak, A.; Li, B.; Sebti, S.; Guida, W.; Schönbrunn, E.; Chen, J. *J. Biol. Chem.* **2010**, *285*, 2174.
12. Our molecular dynamic simulation revealed that the pyrazoline cross-linker shows a bimodal distribution, with the terminal C–C distance spanning from 4.0 Å to 11.6 Å, making it suitable for both *i*, *i*+4 and *i*, *i*+7 stapling: See Figure S5 in Supplementary data for details.
13. Smith, B. A.; Daniels, D. S.; Coplin, A. E.; Jordan, G. E.; McGregor, L. M.; Schepartz, A. *J. Am. Chem. Soc.* **2008**, *130*, 2948.
14. (a) García-Echeverría, C.; Chène, P.; Blommers, M. J.; Furet, P. *J. Med. Chem.* **2000**, *43*, 3205; (b) Kallen, J.; Goepfert, A.; Blechschmidt, A.; Izaac, A.; Geiser, M.; Tavares, G.; Ramage, P.; Furet, P.; Masura, K.; Lisztwan, J. *J. Biol. Chem.* **2009**, *284*, 8812.
15. Bird, G. H.; Bernal, F.; Pitter, K.; Walensky, L. D. *Methods Enzymol.* **2008**, *446*, 369.